Penerbit Akademia Baru

Journal of Advanced Research in Numerical Heat Transfer

Journal homepage:
https://www.akademiabaru.com/submit/index.php/arnht/index
ISSN: 2735-0142

Marangoni Convection in Liquid Bridges due to a Heater/Cooler Ring

Manoj Kumar Tripathi[1,*], Aadil Hashim Saifi[1]

[1] Department of Chemical Engineering, IISER Bhopal, Bhopal 462 066, Madhya pradesh, India

ARTICLE INFO

Article history:
Received 22 December 2022
Received in revised form 18 January 2023
Accepted 21 February 2023
Available online 20 March 2023

Keywords:
Thermocapillary convection; Marangoni flow; liquid-bridge; pinned contact line

ABSTRACT

Liquid-liquid systems in contact with solids often give rise to the formation of liquid bridges. Such geometries generated by fluids are exploited in a variety of scenarios ranging from specialized rheometers to silicon crystal production. The presence of immiscible fluid-fluid interfaces and thermal, solutal or electric field gradients cause such systems to exhibit Marangoni effects. In the present study, we have chosen a capillary bridge of water bounded by two solid insulated discs surrounded by silicone oil. This liquid bridge has been subjected to a heater or cooler ring around it. We study the fluid dynamics and heat transfer due to the ring for different heater/cooler locations. We observe drastic differences between heater and cooler configurations in terms of the maximum interfacial velocities, net heat transferred to the bridge and location of the stagnation points. Flow and bridge shape is seen to be more stable in the cooler ring cases. Anomalous results for heat transfer rate, interface deformation and circulation patterns are obtained in the heater configuration for larger height to radius ratios. Moreover, when the heater/cooler ring is placed close to the solid discs, anomalous dynamics is observed.

1. Introduction

Liquid bridges appear when a pocket of a fluid is trapped between solids in the presence of another immiscible fluid. Such a scenario may appear in several industrial as well as natural settings, such as underground oil recovery [1], packed- bed reactors [2], and binder-jet printing [3]. Liquid bridge geometry offers a way for two immiscible fluids to coexist within a porous solid. Several analytical studies have been conducted in the past to derive the shapes of the liquid bridges as well the forces that are applied by the bridge [4, 5]. In most of the practical situations, often there are thermal or solutal gradients present in the system which cause the Marangoni forces to play a role in the dynamics of the liquid bridges. Marangoni forces may cause delayed coalescence of droplets on a pool [6], or cause an otherwise partial coalescence to convert to a total coalescence [7]. Moreover, thermal gradients may deteriorate the crystal quality in a float-zone process [8]. Therefore, Marangoni forces in liquid bridges with gravitational effects require a detailed investigation. Most of the earlier studies have focussed on cylindrical liquid bridge geometries without considering the interface deformation [9], which limits the applicability of such studies to low Weber number regimes. In the presence of gravity, the liquid bridge may itself be vertically asymmetric for larger

* *Corresponding author.*
E-mail address: manojkt@iiserb.ac.in (Manoj Kumar Tripathi)

volumes, and the Marangoni convection in such a geometry may be very different as compared to that in a cylindrical one. In this work, we study the effect of a heating and a cooling ring on a capillary bridge of water surrounded by silicone oil (10 cSt) and bounded by two discs on top and bottom. We investigate the effect of heater/cooler position and bridge aspect ratios on the fluid flow and heat transfer in this system.

2. Materials and Methods

A cylindrical capillary bridge made of water (merck-millipore) held between a top and a bottom insulated disc is allowed to deform under gravity in the presence of a 10 cSt silicone oil. A schematic diagram of the system with various dimensions is shown in Figure 1. The geometrical and flow parameters are similar to the ones considered in our earlier work [10]. The values of these parameters are mentioned in Table 1. An initial temperature difference, ΔT°C is set up between the heater/cooler ring and the liquids, wherein, the positive and negative values of ΔT indicate a heater and a cooler configuration, respectively. The location of the ring, z_q is changed in order to study its effect on the flow dynamics and heat transfer. A cylindrical coordinate system (r, ϑ, z) has been used to solve the governing equations for this system, with the z axis being the axis of symmetry. The gravity acts in the downward ($\_z$) direction. A one-fluid formulation has been employed to solve the mass, momentum and energy conservation equations for an incompressible fluid [7].

$$\nabla \cdot \mathbf{u} = 0, \tag{1}$$

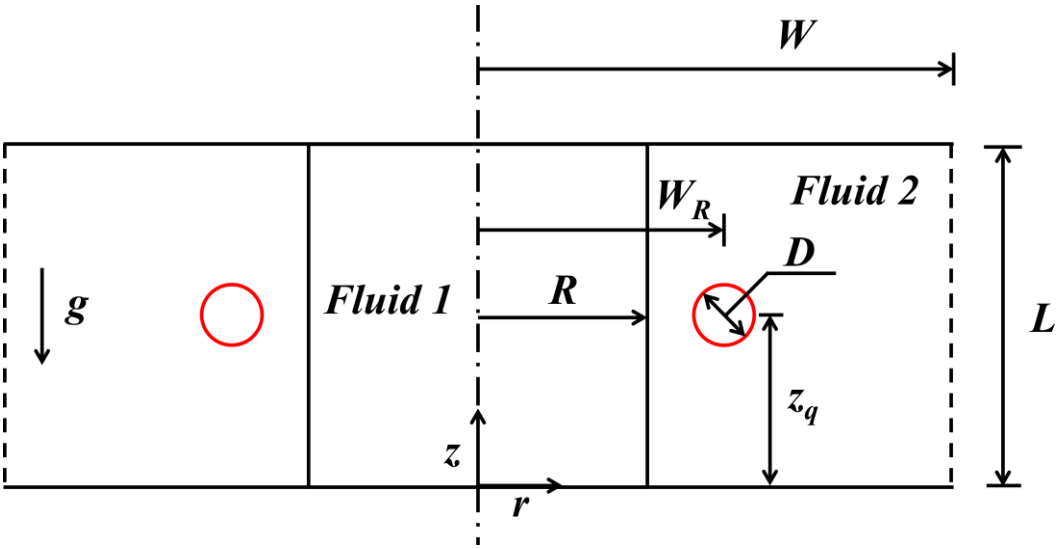

Fig. 1. Schematic diagram of a liquid bridge showing various dimensions. The dash-dotted line represents the axis of azimuthal symmetry, and the dashed lines show the fluid domain boundary. The horizontal, solid, top and bottom lines represent the solid discs, and the heater/cooler ring is shown by the circles outlined in red color

$$\rho(T,c)\left[\frac{\partial \mathbf{u}}{\partial t} + \mathbf{u}\cdot\nabla\mathbf{u}\right] = \nabla\cdot\left[\mu(T,c)(\nabla\mathbf{u} + \nabla\mathbf{u}^T)\right] - \nabla p + \mathbf{F} - \rho(T,c)g\hat{z}, \tag{2}$$

$$\frac{\partial T}{\partial t} + \mathbf{u} \cdot \nabla T = \nabla \cdot [\alpha(T,c)\nabla T], \tag{3}$$

$$\frac{\partial c}{\partial t} + \mathbf{u} \cdot \nabla c = 0, \tag{4}$$

wherein, **u**, p and T are velocity, pressure, and temperature in the entire domain, respectively; t denotes time. F represents a combination of the normal interfacial tension force and the tangential thermocapillary force, defined as $(\delta(\mathbf{x} - \mathbf{x_i})\sigma(T)\kappa\mathbf{n} + \delta(\mathbf{x} - \mathbf{x_i})\nabla_s\sigma(T))$, where, $\delta(\mathbf{x} - \mathbf{x_i})$ is the Dirac-delta function, where $\mathbf{x_i}$ is the position vector of the interface; **n** is the unit normal to the interface pointing towards fluid '2'; the interface curvature, $\kappa = \nabla\ \mathbf{n}$; ∇_s denotes the surface gradient operator; o denotes the interfacial tension coefficient, which is a function of temperature. The density (ρ), viscosity (μ) and thermal diffusivity (α) are considered to be linear functions of the volume fraction, c, as follows,

$$\rho = c\rho_1(T) + (1-c)\rho_2(T), \tag{5}$$

$$\mu = c\mu_1(T) + (1-c)\mu_2(T), \tag{6}$$

where, the densities ρ_1 and ρ_2 are expressed as $\rho_{10}\{1 - \gamma_1(T - T_1)\}$ and $\rho_{20}\{1 - \gamma_2(T - T_1)\}$, respectively, wherein $T_1 = 25^{\circ}$C; γ_1 and γ_2 being the coefficients of thermal expansion, and ρ_{10} and ρ_{20} are the densities at room temperature for the fluids '1' and '2', respectively. Similarly, μ_i and α_i (for i = 1, 2) are the viscosities and thermal diffusivities for fluid 'i', with the functional dependence of the viscosities on temperature similar to that considered in our earlier work [7]. The interfacial tension, σ is assumed to satisfy the following dependence on temperature,

$$\sigma = \sigma_0 - \sigma_T(T - T_1) \tag{7}$$

Where

$$\sigma_T = -\left(\frac{d\sigma}{dT}\right)_{T_1}$$

We employ no-slip and no-pore boundary conditions for velocity at the top, bottom, and the heater/cooler ring boundaries, whereas, a neumann condition for pressure is imposed at these boundaries. A neumann condition for temperature is imposed at the top and the bottom boundaries, while a dirichlet condition, equal to the ring temperature, is imposed at the heater/cooler ring boundary when the heater/cooler is switched on. The numerical method employed here as well its grid convergence and validation study is detailed in our earlier work [10] and the references therein.

Table 1
Geometrical and flow parameters considered for the simulations in the present work

Parameter	Value
L	$2^{(2/3)}$ cm
W	8 cm
R	$2^{(-1/3)}$ cm
W_R	R + 0.2 cm
g	9.8 ms^{-2}
$\rho 1$	997 kg/m^{-3}
$\mu 1$	8.89×10^{-4} Pa.s
$\alpha 1$	1.46×10^{-7} $m^2.s^{-1}$
$\gamma 1$	2.5×10^{-4} $^{\circ}C^{-1}$
$\rho 2$	950 kg/m^{-3}
$\mu 2$	9.5×10^{-3} Pa.s
$\alpha 2$	9.34×10^{-8} $m^2.s^{-1}$
$\gamma 2$	1.07×10^{-3} $^{\circ}C^{-1}$
$\sigma 0$	0.041 $N.m^{-1}$
σT	6×10^{-4} $N.m^{-1}.^{\circ}C^{-1}$

3. Results and Discussion

3.1 Effect of Ar

We consider liquid bridges of three different aspect ratios in this work, i.e. Ar = 0.5, 1 and 2. It is to be noted that there is an upper limit to the aspect ratio for which a liquid bridge may remain stable under gravity. The values considered in this work yield stable liquid bridges. Figure 2 shows the temperature contours and velocity vectors for the three aspect ratios at t = 10s for the cooler and the heater configurations in the left and the right coloumns, respectively. The cases with the lowest bridge aspect ratio, i.e. Ar = 0.5, are expected to have lesser gravitational/buoyancy effects. Therefore, we expect the behaviour near the center of the interface to be similar to the one of the zero gravity cases. When there is no gravity, the flow is expected to be symmetric about the central horizontal plane. Moreover, the interfacial flow is expected to be directed towards the central plane and away from the central plane for the cooler and the heater configurations, respectively. These different flow patterns cause the outer liquid to be pulled towards the interface and repelled from the interface for the heater and the cooler configurations, respectively [10]. This is also visible in Figure 2, the heater case with Ar = 0.5, where the hot outer liquid is seen to be attracted towards the liquid-liquid interface. Such an observation is also made for Ar = 2. As the aspect ratio is increased, the gravitational effects are more prominent. Due to this, the liquid bridge no longer remains in a right cylindrical shape and exhibits a concave and a convex shape in the upper and lower halves of the domain, respectively.

To understand how the flow evolves in the liquid bridge over time, we plot the interfacial velocity extremes, i.e. minimum and maximum, for the abovementioned cases in Figure 3. We observe that all the cases reach a quasi-steady state by approximately t = 10s. The heater cases show a higher interfacial velocity, in general. This may also cause an increased overall convection, leading to a higher heat transfer in the presence of a heater as compared to that for a cooler. For the heater configuration, the extreme interfacial velocities are significantly higher in magnitude when there is no gravity as compared to the cases when the gravitational force is taken into account. This implies that, when the heater is present midway between the two discs, the Marangoni forces geenrated on the interface are opposed by the buoyancy forces to some extent. This may be understood by recalling the fact that

the buoyancy and Marangoni forces oppose each other in the lower half of the domain in the heater cases. On the other hand, the cooler cases do not show such a drastic difference between the maximum interfacial velocities of cases with and without gravity. In the cooler configuration, the gravitational force pulling the colder liquid and the Marangoni force in the bottom half of the domain, act in the same direction. Therefore, the minimum (downward) interfacial velocity has a higher magnitude for the case with gravity. In the upper half of the domain, the flow is governed mostly by the Marangoni forces in the cooler configuration.

Despite it appearing intuitive that heater and cooler configurations produce similar but opposite flow and heat transfer, we observe that there are significant dissimilarities between the two configurations. Now, we move to the study of the effect of the heater/cooler ring position, z_q, as it may give more insights into the differences and similarities between a heater and a cooler configuration for different heater/cooler locations.

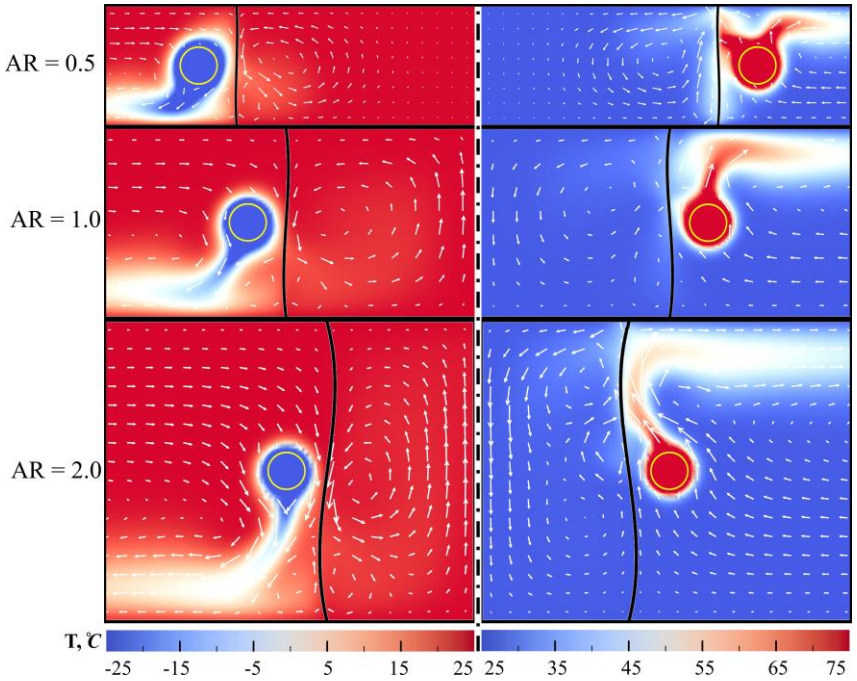

Fig. 2. Temperature contours and streamlines for (a) *Ar* = 2, (b) *Ar* = 1, and (c) *Ar* = 0.5. The left and right coloumns show the plots for the heater and the cooler configurations, respectively

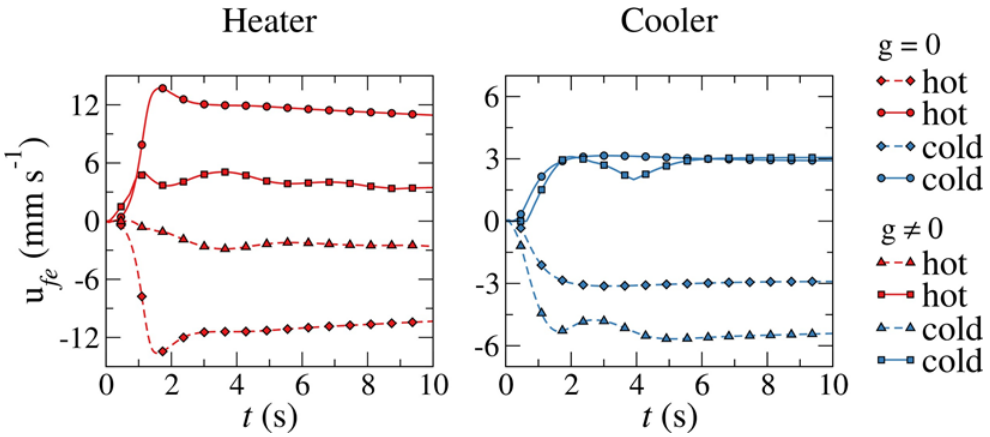

Fig. 3. Plots showing the time evolution of the maximum (upward) and the minimum (downward) velocity on the interface for heater and cooler configurations with ($g \neq 0$) and without ($g = 0$) gravity

3.2 Effect of z_q

To understand the effect of the heater/cooler location we plot the maximum and minimum interfacial velocities for $Ar = 2$, and different heater and cooler locations in Figure 4. We make the following observations for the heater configuration. For most of the z_q values, the interfacial velocity attains a quasi-steady state. The maximum interfacial velocity, $u_{f,max}$, is highest for $z_q = 0.1L$ and $0.3L$. As the heater is lowered, $u_{f,max}$ tends to decrease, and $u_{f,min}$ appears to increase, with some exceptions. This general trend is expected due to the opposing buoyancy force becoming stronger as the heater is lowered. In general, the interfacial velocity for the heater cases is much higher than that for the comparable cooler cases. The interfacial velocity shows a highly unsteady behaviour for the early time, especially in the heater cases. Moreover, the cooler cases attain a quasi-steady state much earlier than the corresponding heater cases. In this respect, $z_q = 0.9L$ is an exception, which may be attributed to the interface shape and wall effects. As shown in Figure 2, the interface shape near the upper disk is concave, whereas it is convex near the lower disk. This causes an asymmetry in the convection and heat transfer rates between the equivalent heater and cooler cases when the heater is near the bottom disk and the cooler is near the top disk. We observe the the extreme interfacial velocity for the cooler position $z_q = 0.1L$, $0.7L$ and $0.9L$. It has been observed that the heat transfer to/from the liquid bridge is directly related to the fluid flow, which is represented by the interfacial velocity. We have observed (not shown here), that the net heat transfer attains an asymptotic value for all the cases. For the heater cases, the net heat transfer to the bridge is larger than the heat transfer from the bridge in the cooler cases. The trend of the net heat transfer with the ring location is similar to that for the extreme interfacial velocity.

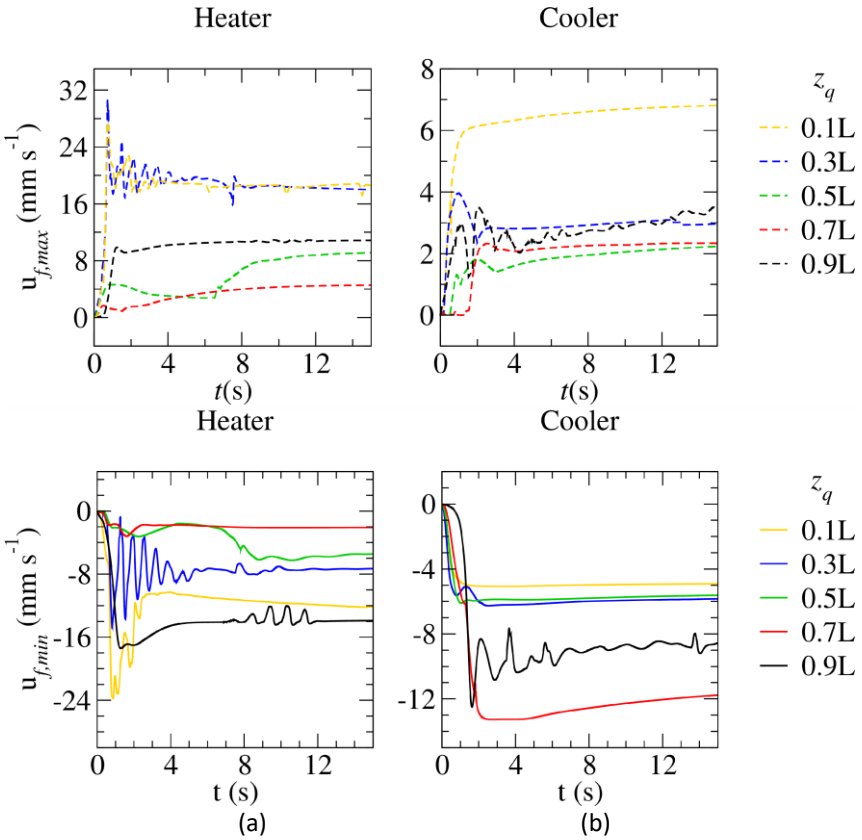

Fig. 4. Comparison of u_Z *vs.* r at different locations of (a) heating (z_h) and (b) cooling (z_C) ring for $\Delta T = 50^{\circ}$C and $Ar = 2$ at $t = 20s$. The fluid properties are as mentioned in Table 1

4. Concluding Remarks

A capillary bridge bounded by two parallel disks in a silicone oil-water system is subjected to a heater/cooler ring around it. The resulting flow and heat transfer is analyzed via two-dimensional axisymmetric simulations incorporating thermo- capillary effects. The effects of the bridge aspect ratio and the heater/cooler location have been studied. A fundamental difference between the heater and cooler configuration is observed even without the presence of gravity. The hot outer fluid is attracted towards the interface and the cold outer fluid is repelled from the interface in the heater and the cooler configu- rations, respectively. As the bridge aspect ratio is increased, the gravitational forces dominate the dynamics. In general, the convection and heat transfer in the heater configuration is significantly higher than that for the cooler cases.

Cooler configurations exhibit a lower interfacial velocity magnitude as compared to that for the heater cases. A bigger, upper recirculation zone is observed in the cooler ₹onfiguration for all cooler locations. The convection has an impact on the heat transfer. The net heat transfer to the liquid bridge is almost equal in magnitude for the lowest heater position and the highest cooler position. However, the net heat transfer falls much more rapidly with respect to the cooler position, when it is lowered, as compared to the heater position when it is moved upwards. The minimum net heat transfer to the inner liquid is shown by the heater case for $z_q = 0.7L$, whereas this occurs at $z_q = 0.5L$ for the cooler configuration. This is attributed to the shape of the liquid bridge which causes a sudden change in the convection pattern at t 8s for $z_q = 0.5L$, in turn increasing the heat transfer rate significantly.

The results presented in this study show differences and similarities between the flow and heat transfer dynamics in liquid bridges which are heated or cooled using a surrounding ring. We hope that this will inspire further work for industrial scenarios where the heat transfer to the bridge is important. Moreover, three-dimensional studies are crucial to test the applicability of the axisymmetric results for the flow regimes considered in this work. We intend to pursue this task in a future work.

References

[1] Saadat, Marzieh, Junyi Yang, Marcin Dudek, Gisle Øye, and Peichun Amy Tsai. "Microfluidic investigation of enhanced oil recovery: The effect of aqueous floods and network wettability." *Journal of Petroleum Science and Engineering* 203 (2021): 108647.

[2] Wu, Zhenyu, Jinjin Cai, Dimiao Wang, Xiaojiang Liang, Qinglong Xie, Yong Nie, and Jianbing Ji. "Hydrodynamics and droplet size distribution of liquid–liquid flow in a packed bed reactor with orifice plates." *AIChE Journal* 67, no. 11 (2021): e17370.

[3] Mostafaei, Amir, Amy M. Elliott, John E. Barnes, Fangzhou Li, Wenda Tan, Corson L. Cramer, Peeyush Nandwana, and Markus Chmielus. "Binder jet 3D printing—Process parameters, materials, properties, modeling, and challenges." *Progress in Materials Science* 119 (2021): 100707.

[4] Delaunay, C. H. "Sur la surface de révolution dont la courbure moyenne est constante." *Journal de mathématiques pures et appliquées* 6 (1841): 309-315.

[5] Orr, F. M., L. E. Scriven, and Ay P. Rivas. "Pendular rings between solids: meniscus properties and capillary force." *Journal of Fluid Mechanics* 67, no. 4 (1975): 723-742.

[6] Geri, Michela, Bavand Keshavarz, Gareth H. McKinley, and John WM Bush. "Thermal delay of drop coalescence." *Journal of Fluid Mechanics* 833 (2017): R3.

[7] Saifi, A. H., and M. K. Tripathi. "Distinct coalescence behaviors of hot and cold drops in the presence of a surrounding viscous liquid." *Physics of Fluids* 32, no. 8 (2020): 082101.

[8] Liu, Yong, Zhong Zeng, Liangqi Zhang, Hao Liu, Yao Xiao, and Yue Wang. "Effect of crystal rotation on the instability of thermocapillary–buoyancy convection in a Czochralski model." *Physics of Fluids* 33, no. 10 (2021): 104101.

[9] Varas, R., P. Salgado Sánchez, J. Porter, J. M. Ezquerro, and V. Lapuerta. "Thermocapillary effects during the melting in microgravity of phase change materials with a liquid bridge geometry." *International Journal of Heat and Mass Transfer* 178 (2021): 121586.

[10] Saifi, A. H., V. M. Mundhada, and M. K. Tripathi. "Thermocapillary convection in liquid-in-liquid capillary bridges

due to a heating/cooling ring." *Physics of Fluids* 34, no. 3 (2022): 032112.